CrossMark

Synthesis and characterization of tungstophosphoric acid-modified mesoporous sponge-like TUD-1 materials

Marina N. Gorsd [iD][1] · Alexis A. Sosa[1] · Romina A. Frenzel[1] · Luis R. Pizzio[1]

Abstract

Mesoporous sponge-like siliceous materials (TUD-1) were synthesized using TEOS (tetraethylorthosilicate) as a precursor of silica and TEA (triethanolamine) as a mesostructure-directing agent. Different TEOS/TEA molar ratios and hydrotreatment times were used, and their influence on the textural and morphological properties of the solids was evaluated. They were characterized by transmission electron microscopy (TEM), X-ray diffraction, and N_2 adsorption/desorption isotherm analysis. By changing the TEOS/TEA molar ratio, micro-mesoporous and mesoporous (with a narrow or wide pore size distribution) materials were obtained. The increment of hydrotreatment times increased the average pore size of TUD-1 and significantly reduced the specific surface area. TEM images showed that the solids were formed by agglomerates of rather spherical particles whose size increased with the increment of the TEA amount used. The structure and morphology of TUD-1 solids modified with tungstophosphoric acid (TPA) were similar to those of the mesoporous silica used as support. Their diffraction patterns did not display any of the characteristic peaks of TPA or its more common hydrates, suggesting that TPA was well dispersed on the support as a noncrystalline phase. In addition, the characterization of all the solids impregnated with TPA by FT-IR and ^{31}P NMR indicated the presence of undegraded $[PW_{12}O_{40}]^{3-}$ and $[H_{3-X}PW_{12}O_{40}]^{X-}$ species interacting electrostatically with the $\equiv Si-OH_2^+$ groups, and by potentiometric titration it was estimated that the solids presented very strong acid sites. The TUD-1 solids modified with TPA gave excellent yield in the solvent-free synthesis of 2,4,5-triphenyl-1H-imidazole, without formation of by-products resulting from competitive reactions or decomposition products. In summary, they are good candidates to be used in multicomponent reactions catalyzed by acids.
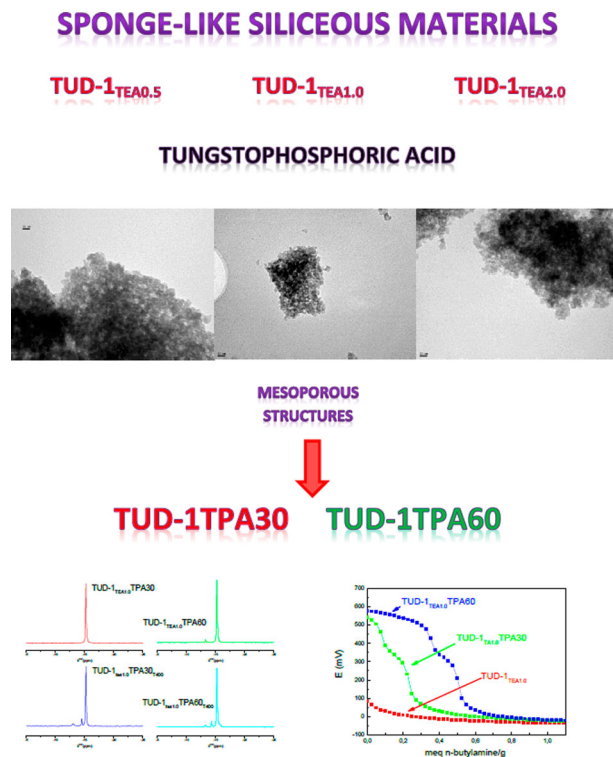
✉ Marina N. Gorsd
  marinagorsd@conicet.gov.ar

✉ Luis R. Pizzio
  lrpizzio@quimica.unlp.edu.ar

[1] Centro de Investigación y Desarrollo en Ciencias Aplicadas "Dr. Jorge J. Ronco" (CINDECA), Departamento de Química, Facultad de Ciencias Exactas, Universidad Nacional de La Plata-CCT La Plata, CONICET, Calle 47N° 257, 1900 La Plata, Argentina

∅ Springer

Graphical Abstract

Highlights

- TUD-1 materials were synthetized using different TEOS/TEA molar ratios and hydrotreatment times.
- Their influence on the textural and morphological properties was evaluated.
- The TUD-1 materials were impregnated with tungstophosphoric acid.
- They gave excellent yield in the in the solvent-free synthesis of 2,4,5-triphenyl-1H-imidazole.

Keywords Mesoporous silica · TUD-1 · Tungstophosphoric acid · Trisubstituted imidazoles

1 Introduction

During the last decades, much has been reported about the synthesis and application of mesoporous materials in different science areas [1, 2]. In catalysis, mesoporous materials with large surface area and high pore volume have proved to be suitable materials to be used as support [1], since they can easily accommodate large molecules [3] such as heteropoly acids (HPA).

A variety of mesoporous materials with controllable pore diameter distribution and large size channels were developed. These features make them particularly useful for transformation processes in fine chemistry where the environmental impact is relevant. Among them, two of the most important are MCM-41 (Mobil Crystalline Materials No. 41) [4–6] and SBA-15 (Santa Barbara Amorphous No. 15) [6].

More recently, the synthesis of a new siliceous material with high surface area values ($>1200\,\mathrm{m^2/g}$) and interconnected mesopores [7] that display a three-dimensional (sponge-like) array has been reported. This material, known as TUD-1 (Technische Universiteit Delft) [8], can be easily modified by the addition of other elements to its structure. This three-dimensional and irregular mesopore structure allows a fast diffusion into and out of TUD-1, making the material an interesting solid for the development of supported catalysts.

This material is easy to prepare, has high thermal stability, and its synthesis does not require any surfactants.

The applications of TUD-1 in the field of catalysis, medicine, and pharmacy are varied. The incorporation of different elements (such as Al, Zr, Fe, Cr, Co, and Cu) in its structure [9–13] was used to prepare heterogeneous catalysts for acid and oxidation reactions.

Our interest in using HPAs as a catalyst in a multicomponent reaction is because heteropoly anions are effectively used in a variety of organic reactions [14, 15] both in homogeneous and heterogeneous systems.

It is well recognized that bulk HPAs are highly soluble in oxygenated solvent (such as water and alcohols) and non-porous materials with a low specific surface area (3–5 m^2/g), which limits their application as unsupported heterogeneous catalysts. Additionally, they present Brønsted acidity stronger than that of many mineral acids (H_2SO_4, HCl) and conventional solid acids such as SiO_2-Al_2O_3, H_3PO_4-SiO_2, zeolites [16]. The interest in preparing HPA-supported catalysts is that in certain reactions they present a better catalytic activity compared to bulk HPAs [17] and they can be recycled and reused, thus tending to achieve green chemistry processes. We have used a great variety of materials as HPAs support, such as silica, zirconia, alumina, carbon, titania, polymeric blends, among others [18–22]. Depending on the preparation method, the TPA interacting with the surface of the support can be partially decomposed, resulting in relatively low acidic materials [23]. On the other hand, it was reported that HPAs are more stable when they are supported on silica [24, 25]. We reported that the acid features of the TPA-support materials prepared by impregnation techniques depend on the nature and stability of the species during impregnation, drying, and calcination steps [26]. We are currently exploring the use of different novel mesoporous siliceous materials, for example, core-shell polystyrene-silica and hollow silica microspheres, as TPA support for the preparation of acid catalysts [14, 27]. The use of mesoporous TUD-1 as HPA support has been scarcely explored [28].

In this work, mesoporous sponge-like siliceous materials (TUD-1) were synthesized using different TEOS/TEA molar ratios and hydrotreatment times, with the purpose of achieving a support with appropriate textural properties to be used as tungstophosphoric acid support. Then, the mesoporous sponge-like material was impregnated with tungstophosphoric acid to obtain materials with appropriate textural and acidic features for further use in the heterogeneously catalyzed synthesis of trisubstituted imidazoles.

2 Materials and methods

2.1 TUD-1 preparation

Silica TUD-1 [8] was synthesized employing SiO_2/TEA/tetraethylammonium hydroxide (TEAOH)/H_2O with the molar ratio 1:X:0.5:1, where X was varied from 0.5 to 2. The obtaining solids will be named TUD-1$_{TEA0.5}$, TUD-1$_{TEA1.0}$, and TUD-1$_{TEA2.0}$, respectively.

A solution of TEA in water was prepared and added to tetraethylorthosilicate (TEOS) solution; to obtain the gel, the mixture was stirred for 2 h. The gel was aged for 24 h at 20 °C and then dried at 100 °C for 24 h. Afterwards, the materials were hydrothermally treated in a Teflon autoclave for a certain fixed time (we used 5, 8, and 12 h) to study the

effect of treatment on the textural properties. Finally, the solids were calcined in air at 600 °C for 10 h, the heating rate being 1 °C/min.

2.2 Impregnation of TUD-1 with tungstophosphoric acid

The mesoporous sponge-like siliceous materials obtained were used as TPA support. The impregnation experiments were performed by contacting, at room temperature, 0.7 g of the support with 0.3 g of tungstophosphoric acid ($H_3PW_{12}O_{40}$) dissolved in 3 ml of ethanol–water 50% (v/v) solution in order to obtain a TPA concentration of 30% by weight in the final material (named TUD-1$_{TEAXX}$TPA30). The same procedure was used to obtain a TPA concentration of 60% (named TUD-1$_{TEAXX}$TPA60). The solution and the support were allowed to stand in contact at room temperature till complete dryness. Finally, the solid was calcined at 400 °C for 2 h under air atmosphere, thus obtaining the solids that will be named TUD-1$_{TEAXX}$TPA30$_{T400}$ and TUD-1$_{TEAXX}$TPA60$_{T400}$, respectively.

The TPA content in the samples was estimated as the difference between the W amount contained in the tungstophosphoric acid solution originally used for the impregnation and the amount of W that remained in the beaker after removing the dried samples. The amount of W in the obtained solutions was determined by atomic absorption spectrometry using a Varian AA Model 240 spectrophotometer. The calibration curve method was used with standards prepared in the laboratory. The analyses were carried out at a wavelength of 254.9 nm, bandwidth 0.3 nm, lamp current 15 mA, phototube amplification 800 V, burner height 4 mm, and acetylene–nitrous oxide flame (11:14). The values measured in the analyzed samples show that practically all of the TPA (more than 97%) contained in the impregnation solution was incorporated into the final materials.

2.3 Characterization

2.3.1 Transmission electron microscopy

The solids were studied by transmission electron microscopy (TEM) in a JEOL 100 CXII microscope, working at 100 kV. The samples were crushed in an agate mortar, ultrasonically dispersed in isobutanol, and deposited on a carbon-coated copper grid.

2.3.2 N$_2$ adsorption–desorption at liquid-nitrogen temperature

The textural properties of the synthesized solids were determined from the adsorption–desorption isotherms at

the temperature of liquid N_2. The isotherms were obtained using the Micromeritics ASAP 2020 equipment. The samples were previously degassed at 100 °C for 2 h. From the obtained data, the specific surface area (S_{BET}), using the Brunauer–Emmett–Teller model in the relative pressure range 0.05–0.3, the mean pore diameter (D_p) by the BJH method, and the pore size distribution (PSD) by the DFT (Density Functional Theory) method, was estimated.

2.3.3 X-ray diffraction

The X-ray diffraction (XRD) patterns were obtained by using the Phillips PW-1732 equipment with built-in recorder. The conditions used were: Cu Kα radiation, Ni filter, 20 mA and 40 kV in the high voltage source, scanning range from 5 to 60° 2θ, and a scanning speed of 1°/min.

The XRD patterns at low angle were acquired using Phillips APD 1700 XPERT, Cu Ka radiation, 40 mA and 40 Kv in the voltage source, scanning range between 0.3 and 5° 2θ, and scanning speed of 0.01° 2θ/s. A PW3011/20 detector was used.

2.3.4 Fourier transform infrared spectroscopy

The Fourier transform infrared spectroscopy (FT-IR) spectra of samples were recorded on the Bruker IFS 66 equipment. Pellets of ca. 1% w/w of the sample in KBr were prepared in a self-made device. A wavenumber range of 400–4000 cm^{-1} was studied, the resolution being 2 cm^{-1}.

2.3.5 Potentiometric titration with *n*-butylamine

The acidic properties of solids were estimated by potentiometric titration with *n*-butylamine. To this end, 50 mg of solid suspended in 45 cm^3 acetonitrile was stirred for 3 h. Then, the titration was carried out with a solution of *n*-butylamine in acetonitrile (0.05 N) using a Metrohm 794 Basic Titrino apparatus with a double-junction electrode.

2.3.6 Nuclear magnetic resonance

The TUD-1$_{TEAXX}$TPA30 and TUD-1$_{TEAXX}$TPA60 samples, before and after being calcined at 400 °C, were analyzed by ^{31}P magic angle spinning-nuclear magnetic resonance (MAS-NMR) spectroscopy. For this purpose, the Bruker MSL-300 equipment was employed, using 5 ms pulses, a repetition time of 3 s, and working at a frequency of 121.496 MHz for 31P at room temperature, the resolution being 3.052 Hz per point. A 5 mm diameter and 10 mm high sample holder were used; the spin rate was 2.1 kHz. Several hundred pulse responses were collected. Phosphoric acid 85% was employed as an external reference.

2.4 Catalytic evaluation

The synthesis of 2,4,5-triphenyl-1*H*-imidazole was carried out in a batch reactor, which was immersed in an oil bath with temperature control using a benzyl:benzaldehyde:ammonium acetate molar ratio of 1:1:1.2 and the amount of TUD-1$_{TEAXX}$TPA30$_{T400}$ (or TUD-1$_{TEAXX}$TPA60$_{T400}$) containing 0.01 mmol of TPA, in the absence of solvent. The mixture was heated up to 130 °C for 60 min.

After the reaction time was reached, the obtained solid was washed twice with 2 cm^3 of distilled water, and the solvent was evaporated in a vacuum oven to concentrate the reaction mixture up to constant weight at room temperature. Then, product separation was performed by means of three extractions with 2 cm^3 of solvent, leaving the catalyst as a solid phase, which was then dried at 40 °C in a vacuum oven.

The organic extracts were dried and concentrated in a vacuum oven at room temperature. The residue was purified by recrystallization using ethanol as the recrystallization solvent. The percentage yield for each case was calculated as the percentage of the product/reactive molar ratio.

The product obtained was identified by 1H and 13C nuclear magnetic resonance (NMR) spectroscopy. 1H and 13C NMR spectra were recorded on a Bruker Avance II 500 at 500.13 and 125.77 MHz, respectively, in DMSO-d6, unless indicated otherwise. Chemical shifts are given in ppm downfield from TMS as an internal standard, and *J* values are given in Hz.

3 Results and discussion

The N_2 adsorption–desorption isotherms of the materials synthesized employing a SiO_2/TEA molar ratio equal to 0.5, 1.0, and 2.0 (TUD-1$_{TEA0.5}$, TUD-1$_{TEA1.0}$, and TUD-1$_{TEA2.0}$, respectively) are shown in Fig. 1. According to IUPAC, the isotherms can be classified as type IV, characteristic of mesoporous materials, and they present type H2 hysteresis.

H1 and H2 type hysteresis loops are observed for solids consisting of particles crossed by nearly cylindrical channels or made by aggregates of spheroidal particles. In both cases, pores can have uniform size and shape (type H1) or nonuniform size or shape (type H2) [29].

The specific surface area (S_{BET}) together with the mean pore diameter (D_p), the total pore volume (V_p) estimated from the value corresponding to a $P/P_0 = 0.98$, and the PSD obtained using the DFT method, the micropore specific surface area (S_{micro}) and volume (V_{micro}) estimated by the *t*-plot method [30, 31] are listed in Table 1.

The mean pore diameter (D_p) of TUD-1$_{TEA0.5}$, TUD-1$_{TEA1.0}$, and TUD-1$_{TEA2.0}$ is higher than 4.0 nm, and increases with the increment of the TEA amount used.

Fig. 1 N_2 adsorption–desorption isotherms of TUD-1$_{TEA0.5}$, TUD-1$_{TEA1.0}$, and TUD-1$_{TEA2.0}$ materials
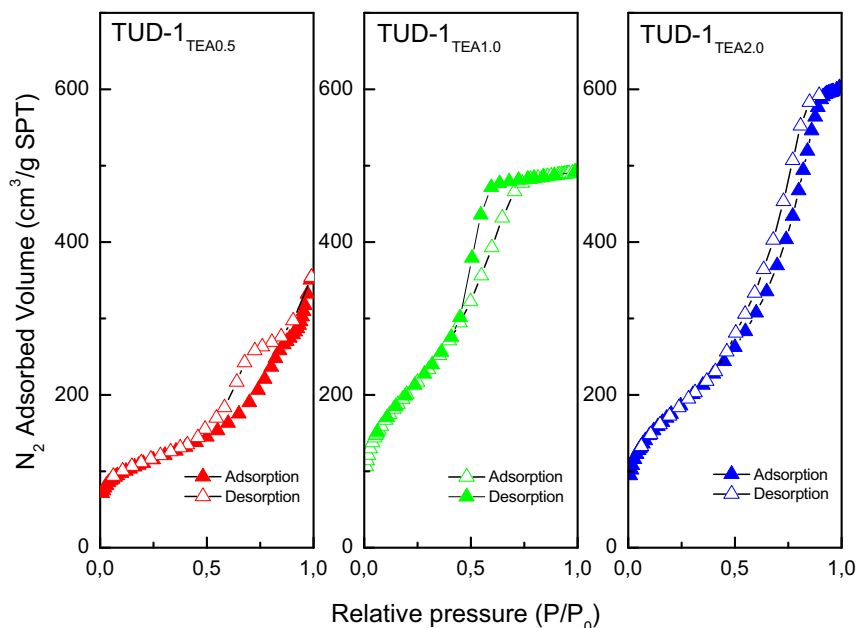

Table 1 Textural properties of TUD-1 solids synthesized under different conditions and impregnated with different concentrations of TPA

Sample	S_{BET} (m²/g)	S_{Micro} (m²/g)	V_p (cm³/g)	V_{micro} (cm³/g)	D_p (nm)
TUD-1$_{TEA1.0}$	719	–	0.76	–	4.2
TUD-1$_{TEA0.5}$	391	112	0.54	0.05	5.5
TUD-1$_{TEA2.0}$	625	7	0.93	–	5.9
TUD-1$_{TEA1.0}$T8h	440	26	0.93	0.01	8.5
TUD-1$_{TEA1.0}$T12h	393	21	0.91	0.01	9.3
TUD-1$_{TEA1.0}$TPA30	429	35	0.44	0.01	4.1
TUD-1$_{TEA1.0}$TPA30$_{T400}$	295	28	0.32	0.01	4.3
TUD-1$_{TEA1.0}$TPA60	209	73	0.17	0.03	3.6
TUD-1$_{TEA1.0}$TPA60$_{T400}$	197	58	0.18	0.02	3.6
TUD-1$_{TEA0.5}$TPA30	165	81	0.33	0.10	5.2
TUD-1$_{TEA2.0}$TPA30	245	42	0.58	0.04	5.8
TUD-1$_{TEA0.5}$TPA60	124	59	0.25	0.05	4.8
TUD-1$_{TEA2.0}$ TPA60	174	36	0.34	0.02	5.5
TUD-1$_{TEA0.5}$TPA30$_{T400}$	135	22	0.27	0.03	5.9
TUD-1$_{TEA0.5}$TPA60$_{T400}$	107	19	0.19	0.04	5.9
TUD-1$_{TEA2.0}$TPA30$_{T400}$	182	41	0.33	0.02	5.8
TUD-1$_{TEA2.0}$TPA60$_{T400}$	146	29	0.26	0.02	5.7

The total pore volume (V_p) also increases with that increment, and it is mainly due to the presence of mesopores. The specific micropore area values (S_{micro}), estimated from the *t*-plot method, show that only in the case of TUD-1$_{TEA0.5}$ sample, the presence of micropores is significant. TUD-1$_{TEA1.0}$ presents the highest S_{BET} value (719 m²/g) and a narrow PSD with maximum at 4 nm (Fig. 2).

In the case TUD-1$_{TEA0.5}$ and TUD-1$_{TEA2.0}$ samples, the PSD reveals a bimodal mesopore structure (with maximum at 4 and 6 nm) and the presence of large mesopores (between 5 and 15 nm) (Fig. 2). However, the specific surface area of TUD-1$_{TEA2.0}$ is rather similar (only 15% lower than TUD-1$_{TEA1.0}$ S_{BET} value) and displays a higher D_p value.
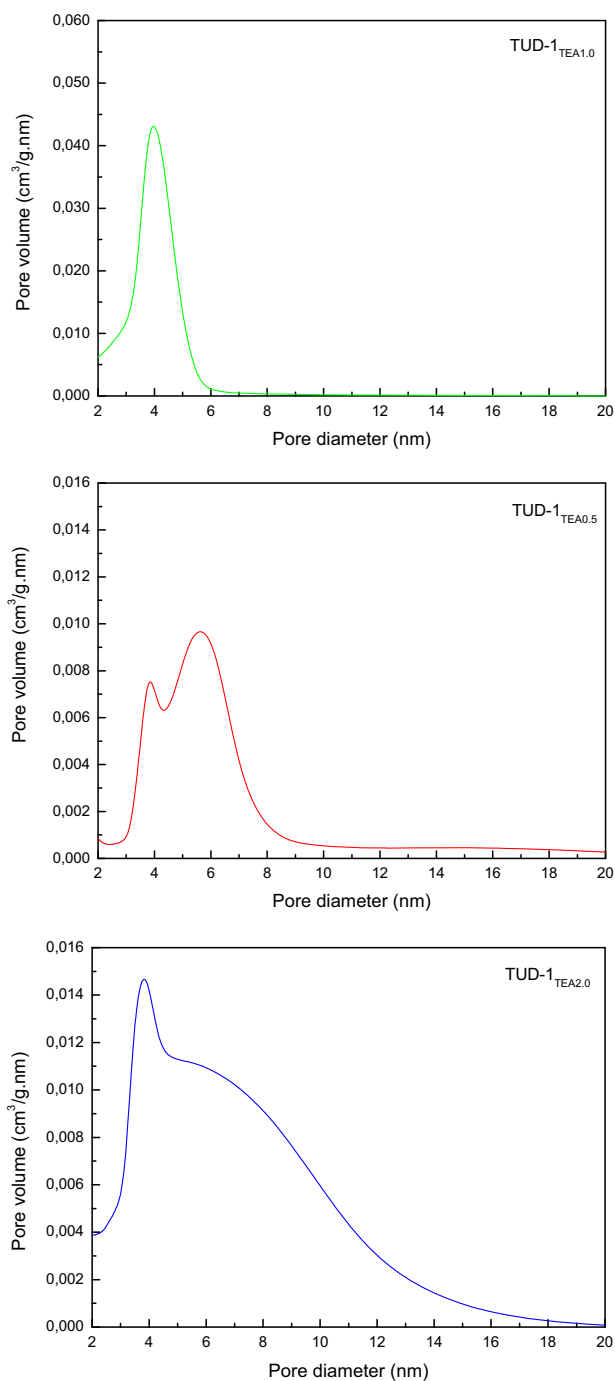
Fig. 2 Pore size distribution of TUD-1$_{TEA0.5}$, TUD-1$_{TEA1.0}$, and TUD-1$_{TEA2.0}$ materials

As a result of the use hydrotreatment times longer than 5 h, the average pore size of siliceous material increases significantly. For example, in the case of TUD-1$_{TEA1.0}$ D_p rises from 4.2 to 8.5 and 9.3 nm when hydrotreatment times increase from 5 to 8 and 12 h, respectively (Table 1). The PSD of TUD-1$_{TEAT8h}$ and TUD-1$_{TEAT12h}$ (Fig. 3) shows mesopores in the range 3–16 and 3–20 nm, respectively. These results are in agreement with those previously

reported by Jansen et al. [8, 32], showing that the pore size can be controlled by modifying the hydrotreatment time.

The specific surface area of the TPA impregnated materials (TUD-1$_{TEAXX}$TPA30 and TUD-1$_{TEAXX}$TPA60) gradually decreases with the increment of the heteropolyacid content (30% and 60%, respectively). On the other hand, TPA incorporation causes a slight change of both D_p and PSDs. The S_{BET} decrement is mainly associated with the proportion of TUD-1 in TUD-1$_{TEAXX}$TPA30 and TUD-1$_{TEAXX}$TPA60 materials (70% and 40%, respectively) (Table 1). In addition, it could also be due to the partial blocking of the TUD-1$_{TEAXX}$ mesopores by the incorporated TPA anion, and therefore the appearance of microporosity. An additional decrease of both S_{BET} and D_p values takes place as a result of the thermal treatment at 400 °C.

The XRD patterns of TUD-1$_{TEA1.0}$TPA30 and TUD-1$_{TEA1.0}$TPA60 (Fig. 4) showed similar characteristics to those of the support (TUD-1$_{TEA1.0}$) used for their preparation. These materials do not display any of the characteristic peaks of TPA or its more common hydrates [27], suggesting that TPA is well dispersed on the support as a noncrystalline phase or present as crystals with a size not detectable by this technique. The study of the calcined solids by XRD displayed quite similar patterns.

Additionally, TUD-1 siliceous material synthesized by varying the TEA concentration and the hydrothermal time exhibits an XRD diagram with the same main features as that of TUD-1$_{TEA1.0}$.

Figure 5 shows the low-angle XRD diffraction patterns of TUD-1$_{TEA1.0}$, TUD-1$_{TEA1.0}$TPA30, and TUD-1$_{TEA1.0}$ TPA30$_{T400}$. They reveal the presence of a broad diffraction peak centered at ~0.8° of 2θ, characteristic of the no ordered three-dimensional mesopore structure of these materials [33]. They also show that the impregnation and calcination at 400 °C do not significantly affect the mesoporous structure, in concordance with D_p reported values (Table 1).

TEM images of TUD-1$_{TEA0.5}$, TUD-1$_{TEA1.0}$, and TUD-1$_{TEA2.0}$ (Fig. 6) show that the solids are formed by agglomerates of rather spherical particles. The size of these particles in the range 5 and 10 nm decreases with the increment of the TEA amount used. The TEM images of TUD-1$_{T8h}$ and TUD-1$_{T12h}$ samples do not show any remarkable modification of the size as a result of the increment of the hydrothermal treatment. On the other hand, TEM images of TUD-1$_{TEAXX}$TPA30$_{T400}$ and TUD-1$_{TEAXX}$ TPA60$_{T400}$ reveal that the sponge-like mesoporous structure characteristic of TUD-1 remains unchanged after the impregnation and calcination of the materials.

The FT-IR characterization of TUD-1$_{TEA1.0}$ (Fig. 7a) showed the characteristic silica bands placed at 3700–3200 (stretching of OH groups), 1650 (angular vibration of H_2O), 1091 (asymmetric stretching of the siloxane group), 977 (stretching of the Si–OH group), 819 (stretching of the

Fig. 3 Pore size distribution of TUD-1$_{T8h}$ and TUD-1$_{T12h}$ materials
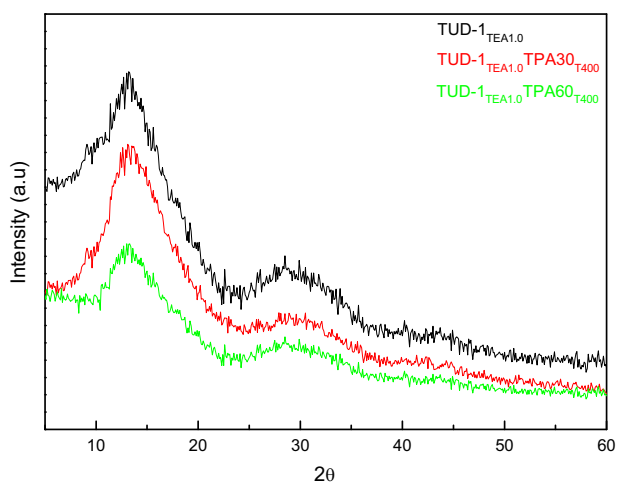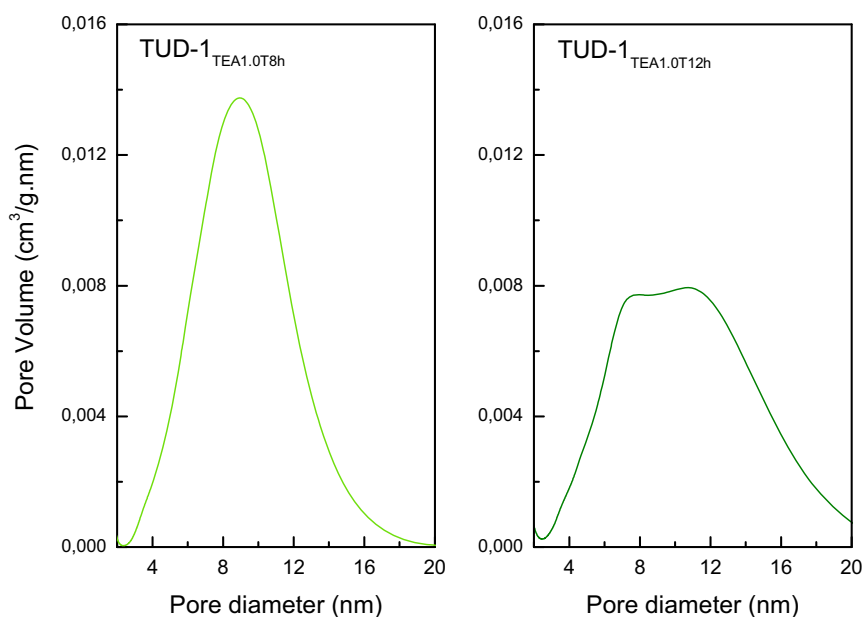
Fig. 4 Diffraction patterns of TUD-1$_{TEA1.0}$, TUD-1$_{TEA1.0}$TPA30, and TUD-1$_{TEA1.0}$TPA60
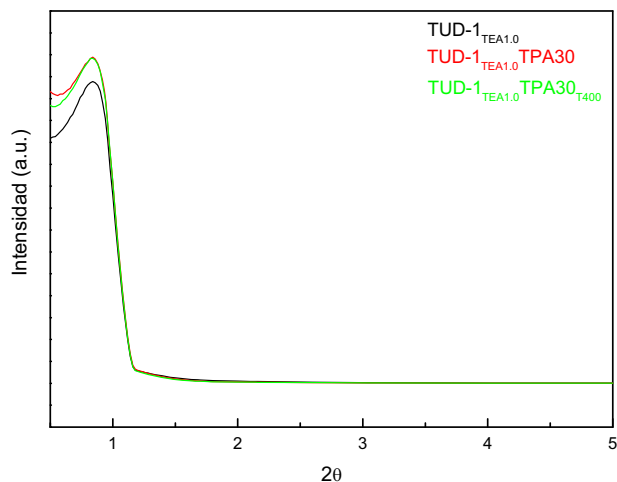
Fig. 5 Low-angle diffraction patterns of TUD-1, TUD-1TPA30, and TUD-1TPA30$_{T400}$

Si–O-Si group), and 465 cm^{-1} (bending of the O-Si–O group) that agree well with those reported in the literature [34].

The absence of the most intense characteristic bands belonging to TEA (bending of N–H and C–N stretching) indicates its complete removal during the calcination at 600 °C.

No remarkable differences were detected from the comparison of TUD-1 FT-IR spectrum with those of samples prepared using different SiO$_2$/TEA molar ratios (Fig. 7a) and hydrotreatment times.
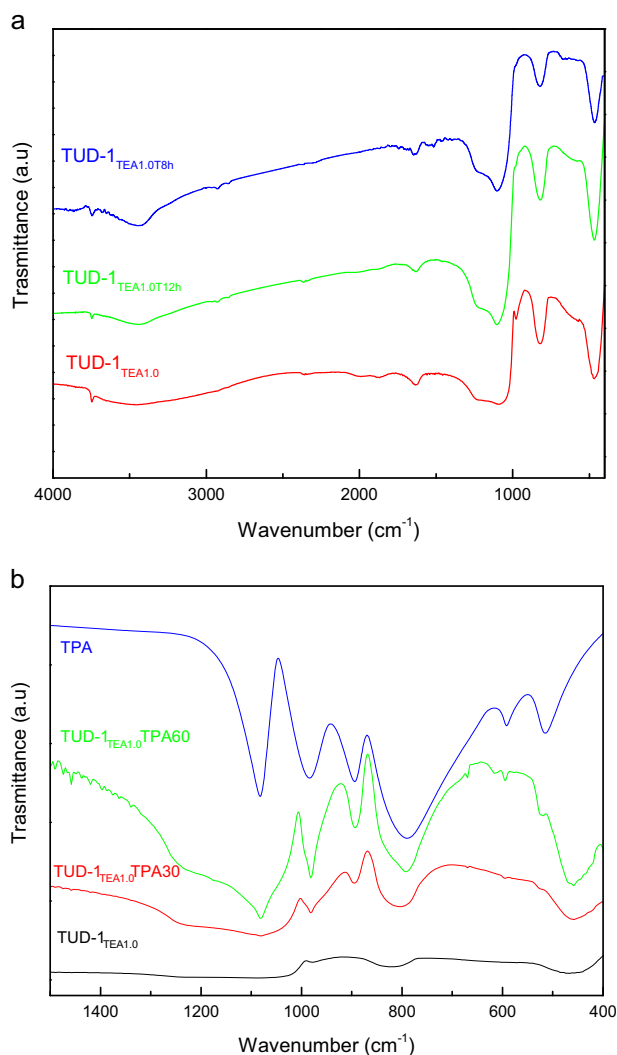
The FT-IR spectra of TUD-1$_{TEA1.0}$TPA30 and TUD-1$_{TEA1.0}$TPA60 (Fig. 7b) solids show that the bands of TPA assigned to the P-Oa, W-Od, and W-Ob-W vibration appear

(at 1080, 981, and 891 cm^{-1} respectively) partially overlapped with the silica bands [35], indicating the presence of the tungstophosphate anion [PW$_{12}$O$_{40}$]$^{3-}$ with Keggin structure. It is necessary to mention that Oa indicates oxygens bridging W placed in the four triads of the octahedra and the P heteroatom of the central tetrahedron that form the Keggin heteropolyanion primary structure, Ob corresponds to oxygens linking the triads through corners, Oc designates edge-sharing oxygens, and Od denotes terminal oxygens [36].

The main features of the FT-IR spectra of calcined samples (TUD-1TPA30$_{T400}$ and TUD-1TPA60$_{T400}$) resemble those of TUD-1$_{TEA1.0}$TPA30 and TUD-1$_{TEA1.0}$TPA60, indicating that no detectable transformation of the Keggin
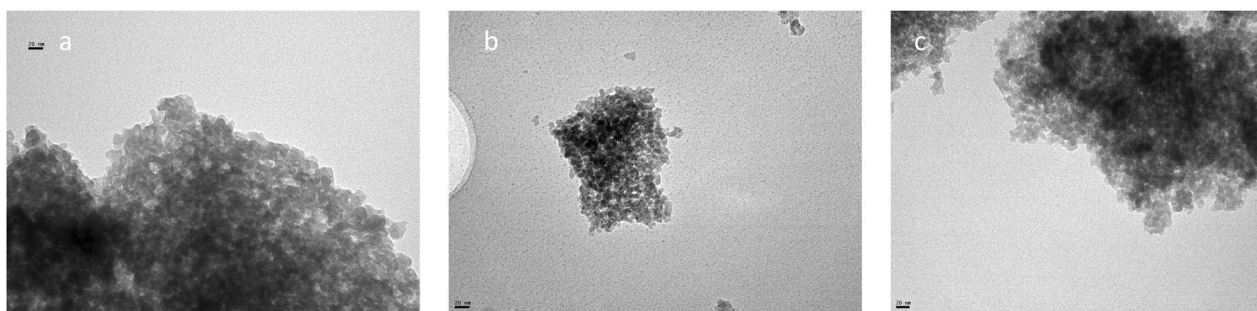
**Fig. 6** TEM micrographs: TUD-1$_{TEA0.5}$ (a), TUD-1$_{TEA1.0}$ (b), TUD-1$_{TEA2.0}$ (c); bar: ×270,000

Fig. 7 **a** FT-IR spectra of solids TUD-1$_{TEA1.0}$, TUD-1$_{TEAT8h}$, and TUD-1$_{TEAT12h}$. **b** FT-IR spectra of solids TUD1, TUD-1TPA30, and TUD-1TPA60

structure takes place due to the treatment at 400 °C. These results are in agreement with the previously reported thermal stability of TPA [37]. They showed (see supplementary material) that the calcination of bulk TPA till 400 °C does not produce any change in the primary structure ($H_3PW_{12}O_{40}$).

The ^{31}P MAS-NMR spectrum of bulk hydrated TPA ($H_3PW_{12}O_{40}.6H_2O$) exhibits only one peak at -15.3 ppm with a small line width. This peak was assigned to the deprotonated $[PW_{12}O_{40}]^{3-}$ Keggin anion [38] that interacts with $H^+(H_2O)_2$ species [39]. This peak was present at -15.2 ppm in the ^{31}P MAS-NMR spectrum corresponding to TUD-1$_{TEA1.0}$TPA30 and TUD-1$_{TEA1.0}$TPA60 samples. The ^{31}P MAS-NMR spectra of TUD-1TPA60 sample also reveal the presence of a very small band at -13.3 ppm, ascribed to the $[P_2W_{21}O_{71}]^{6-}$ anion (Fig. 8).

On the other hand, the ^{31}P MAS-NMR spectra of the same samples after the calcination at 400 °C revealed the presence of the characteristic band of $[PW_{12}O_{40}]^{3-}$ (the most intense) and $[P_2W_{21}O_{71}]^{6-}$ (very small and wide) anion together with a new one at -14.5 ppm assigned to $[H_{3-X}PW_{12}O_{40}]^{X-}$ anions [40, 41]. The increase of the line width observed, compared to the TPA is assigned to the electrostatic interaction among the anions and the $\equiv Si-OH_2^+$ (due to the transfer of protons to silanol groups) species present in TUD-1$_{TEAXX}$TPA samples, similarly to what has been proposed for TPA-titania and TPA-zirconia samples [42, 43]. The calcination of TUD-1$_{TEAXX}$TPA materials produces the release of water molecules from $H^+(H_2O)_2$ species and the formation of $[H_{3-X}PW_{12}O_{40}]^{X-}$ anions, according with:

$$[PW_{12}O_{40}]^{3-} + H^+(H_2O)_2 + \equiv SiOH \rightarrow (\equiv SiOH_2)^+[H_{3-X}PW_{12}O_{40}]^{X-} + 2H_2O.$$
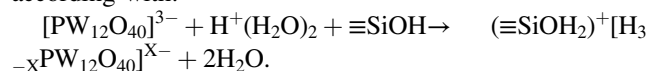
It is possible to estimate the strength and the number of acid sites using potentiometric titration with *n*-butylamine. E_i (the initial electrode potential) indicates the maximum strength, considering that values of $E_i > 100$ mV correspond to very strong sites, values of E_i in the range 100–0 mV to strong sites, and values lower than 0 mV to weak and very weak sites [44]. The area under the curve provides an estimation of the number of acid sites (N_{AS}). This method has been widely employed to measure the number and strength of acid sites in different kind of materials. The goodness of the potentiometric titration was probed using
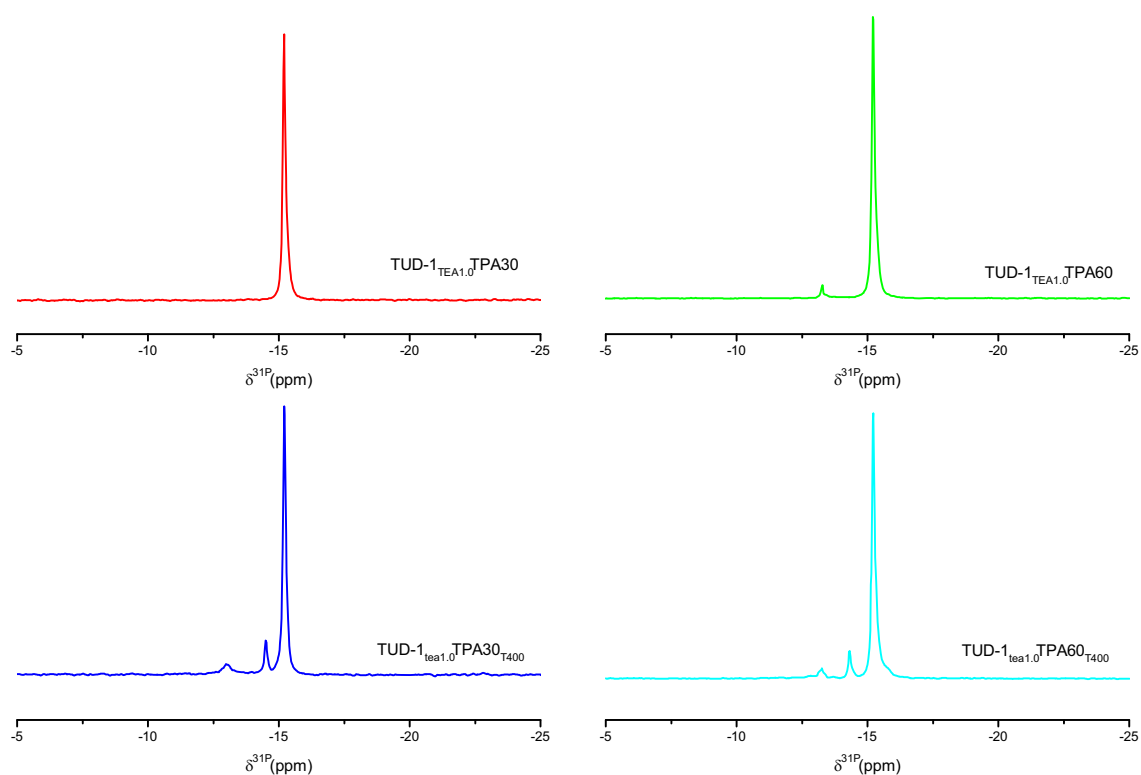
Fig. 8 ^{31}P MAS-NMR spectrum of TUD-1$_{TEA1.0}$TPA30, TUD-1$_{TEA1.0}$TPA60, and the same samples after the calcination at 400 °C

the adsorption of indicators, NH$_3$ temperature programed desorption [45], FT-IR spectrum of adsorbed pyridine [46], and cyclohexene dehydration test reaction [47], among others. Reddy et al. [48] reported that the acidity values of tungstophosphoric acid obtained by the potentiometric method are in good agreement with those obtained by the calorimetric and adsorption method. Additionally, we found that the acidic characteristics of the Cs$_{2.9}$H$_{0.1}$PW$_{12}$O$_{40}$, Cs$_{2.6}$H$_{0.4}$PW$_{12}$O$_{40}$, K$_{2.9}$H$_{0.1}$PW$_{12}$O$_{40}$, and K$_{2.5}$H$_{0.5}$PW$_{12}$O$_{40}$ salts obtained using the potentiometric method straightly correlate with those found through the isopropanol dehydration test reaction [49].

The titration curve of TUD-1$_{TEA0.5}$, TUD-1$_{TEA1.0}$ (Fig. 9), and TUD-1$_{TEA2.0}$ show the presence of a low number of acid sites with E_i values in the range 50–100 mV (79, 86, and 89 mV, respectively). As a result of the impregnation of TUD-1$_{TEAXX}$ with TPA, both the acid strength and the number of acid sites increase significantly (Table 2). On the other hand, regardless the TUD-1$_{TEAXX}$ used as support, quite similar E_i and N_{AS} values are obtained for the samples with the same TPA content.

For example, the potentiometric titration results (Fig. 9a) indicate that TUD-1$_{TEA1.0}$TPA30 and TUD-1$_{TEA1.0}$TPA60 present very strong acid sites with similar E_i values (550 and 585 mV, respectively). However, in the case of TUD-1$_{TEA1.0}$TPA60 the total number of acid sites determined by this technique is twice that of TUD-1$_{TEA1.0}$TPA30.

A slight increase of E_i values is observed for the samples calcined at 400 °C (Fig. 9b), which can be due to the elimination of water molecules that were interacting with the H$^+$ of the TPA [36].

The yields obtained from the synthesis of 2,4,5-triphenyl-1H-imidazole using TUD-1$_{TEAXX}$TPA30 and TUD-1$_{TEAXX}$TPA60 materials as catalysts are shown in Table 3. The yield reached under the same reaction conditions without catalyst (catalyst-free) was rather low (12%). The yields attained using TUD-1$_{TEA1.0}$TPA30$_{T400}$ and TUD-1$_{TEA1.0}$TPA60$_{T400}$ (61% and 96%, respectively) were higher than that reached using bulk TPA (39%). Taking into account that TPA also presents very strong acid sites (E_i = 620 mV), these results can be due to its lower specific surface area (S_{BET} = 2 m^2/g). On the other hand, TUD-1$_{TEA1.0}$TPA60$_{T400}$ displayed a better catalytic performance than TUD-1$_{TEA1.0}$TPA30$_{T400}$ as a result of its higher number of acid sites and acid strength. A similar behavior was observed for the TUD-1$_{TEA0.5}$ and TUD-1$_{TEA2.0}$ based materials. The higher 2,4,5-triphenyl-1H-imidazole yield was obtained with the solid with higher TPA content (Table 3, entries 2 and 6).

When samples with a particular TPA content are considered (e.g., TUD-1$_{TEA0.5}$TPA60$_{T400}$, TUD-1$_{TEA1.0}$TPA60$_{T400}$, and TUD-1$_{TEA2.0}$TPA60$_{T400}$) the yield slightly increased in parallel (TUD-1$_{TEA0.5}$TPA60$_{T400}$ < TUD-1$_{TEA1.0}$TPA60$_{T400}$ < TUD-1$_{TEA2.0}$TPA60$_{T400}$) with
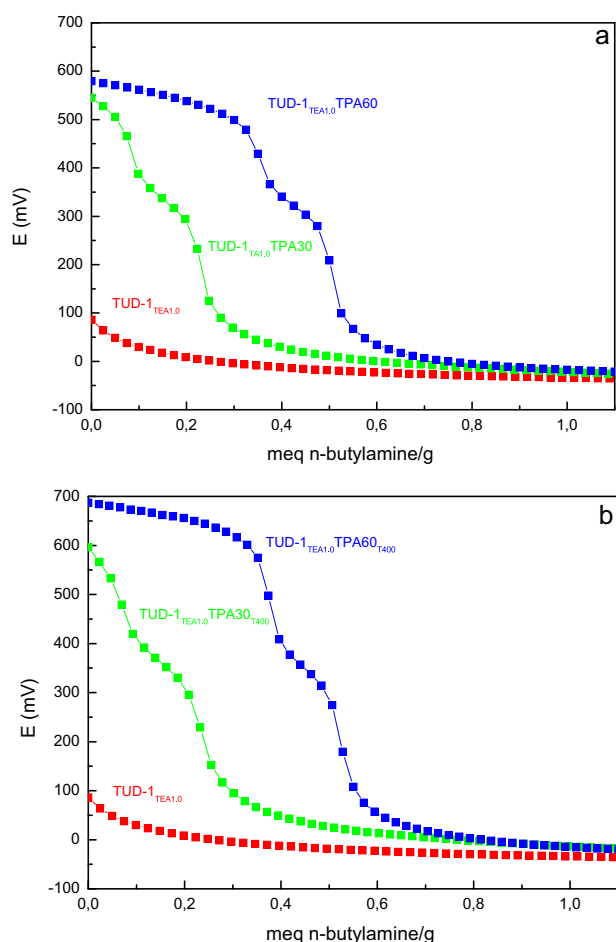
Fig. 9 Potentiometric titration curves of the TUD-1, TUD-1TPA30, and TUD-1TPA60 samples, dried (**a**) and calcined at 400 °C (**b**)

Table 2 Acidic properties of TUD-1 solids synthesized under different conditions and impregnated with different concentrations of TPA

Sample	E_i (mV)	N_{AS}
TUD-1$_{TEA0.5}$TPA30	532	92
TUD-1$_{TEA0.5}$TPA30$_{T400}$	563	109
TUD-1$_{TEA1.0}$TPA30	550	97
TUD-1$_{TEA1.0}$TPA30$_{T400}$	596	113
TUD-1$_{TEA2.0}$TPA30	540	94
TUD-1$_{TEA2.0}$TPA30$_{T400}$	589	110
TUD-1$_{TEA0.5}$TPA60	580	200
TUD-1$_{TEA0.5}$TPA60$_{T400}$	674	235
TUD-1$_{TEA1.0}$TPA60	585	205
TUD-1$_{TEA1.0}$TPA60$_{T400}$	687	245
TUD-1$_{TEA2.0}$TPA60	572	198
TUD-1$_{TEA2.0}$TPA60$_{T400}$	678	240

the increment of the S_{BET} values (Table 2). This statement is in agreement to our previous results [14]. They showed that higher reaction times [90 min] were necessary to obtain

Table 3 2,4,5-Triphenyl-1H-imidazole synthesis employing TUD-1$_{TEAXX}$TPA30$_{T400}$ and TUD-1$_{TEAXX}$TPA60$_{T400}$ materials as catalysts

Entry	Catalyst	Yield (%) to
1	TUD-1$_{TEA0.5}$TPA30$_{T400}$	53
2	TUD-1$_{TEA0.5}$TPA60$_{T400}$	73
3	TUD-1$_{TEA1.0}$TPA30$_{T400}$	69
4	TUD-1$_{TEA1.0}$TPA60$_{T400}$	96
5	TUD-1$_{TEA2.0}$TPA30$_{T400}$	58
6	TUD-1$_{TEA2.0}$TPA60$_{T400}$	81

Reaction conditions: benzyl (1 mmol), aldehyde (1 mmol), ammonium acetate (1.2 mmol), catalyst (1% mmol) without solvent for 60 min at 130 °C

similar yields when the reaction was catalyzed by tungstophosphoric acid supported on core-shell polystyrene-silica microspheres samples with similar acid features but lower S_{BET} values.

Additionally, it is noteworthy to mention that in none of the experiments performed, by-products were formed, indicating that TUD-1$_{TEAXX}$TPA30 and TUD-1$_{TEAXX}$TPA60 catalysts are highly selective.

In summary, TUD-1 materials with suitable properties to be used as heteropolyacid support were synthesized. The impregnation of these sponge-like mesoporous silica materials with tungstophosphoric acid allowed maintaining the Keggin structure of the acid, thus leading to high acidic materials, appropriate to be used in the acid catalyzed synthesis of 2,4,5-triphenyl-1H-imidazole.

4 Conclusions

Silica materials with sponge-like mesoporous structure were prepared using TEA as a non-surfactant and low-cost structure-directing agent, which led to the development of mesoporosity in the material during the polycondensation of inorganic species. The SiO$_2$/TEA molar ratio, which was varied using different amounts of TEA, influenced the specific surface area, PSD, and the presence or absence of micropores. TUD-1 materials with a narrow (in the range 4–6 nm) or wide (in the range 4–16 nm) mesopore size distribution can be easily tuned by varying the SiO$_2$/TEA molar ratio. The use of hydrotreatment times longer than 5 h increased the average pore size of TUD-1 and significantly reduced the specific surface area.

Based on the ^{31}P MAS-NMR and FT-IR results, we concluded that the undegraded $[PW_{12}O_{40}]^{3-}$ anion was the majority species present in all the TUD-1TPA materials, together with $[H_{3-X}PW_{12}O_{40}]^{(3-X)-}$ in the ones treated at 400 °C. Moreover, potentiometric titration showed the presence of very strong acid sites, whose acid strength was almost independent of the TPA content.

Solids based on tungstophosphoric acid impregnated on TUD-1 displayed outstanding textural properties and very strong acidic sites, indicating that the prepared materials will be suitable for their use as acid catalysts in the tri-substituted imidazole by multicomponent reaction.

Compliance with ethical standards

Conflict of interest The authors declare that they have no conflict ofinterest.

References

1. Rivera TS, Sosa A, Romanelli GP, Blanco MN, Pizzio LR (2012) Tungstophosphoric acid/zirconia composites prepared by the sol–gel method: an efficient and recyclable green catalyst for the one-pot synthesis of 14-aryl-14*H*-dibenzo[*a,j*]xanthenes. Appl Catal A Gen 443–444:207–213

2. Rengifo-Herrera JA, Frenzel RA, Blanco MN, Pizzio LR (2014) Visible-light-absorbing mesoporous TiO$_2$ modified with tungstosilicic acid as photocatalyst in the photodegradation of 4-chlorophenol. J Photochem Photobiol A Chem 289:22–30

3. Kozhevnikov IV, Sinnema A, RJJ Jansen, Pamin K, van Bekkum H (1995) New acid catalyst comprising heteropoly acid on a mesoporous molecular sieve MCM-4. Catal Lett 30:241–252

4. Beck JS, Vartuli JC, Kresge CT, Roth WJ, Leonowicz ME, Kresge CT, Schmitt KD (1992) A new family of mesoporous molecular sieves prepared with liquid crystal templates. J Am Chem Soc 114:10834–10843

5. Kresge CT, Leonowicz ME, Roth WJ, Vartuli JC, Beck JS (1992) Ordered mesoporous molecular sieves synthesized by a liquid-crystal template mechanism. Nature 359:710–712

6. Zhao D, Feng J, Huo Q, Melosh N, Fredrickson GH, Chmelka BF, Stucky GD (1998) Triblock copolymer syntheses of mesoporous silica with periodic 50 to 300 angstrom pores. Science 279:548–552

7. Ryoo R, Joo SH, Jun S (1999) Synthesis of highly ordered carbon molecular sieves via template-mediated structural transformation. J Phys Chem B 103:7743–7746

8. Jansen JC, Shan Z, Marchese L, Zhou W, Van der Puil N, aschmeyer T (2001) A new templating method for three-dimensional meso-pore networks Chem Commun 2010:713–714

9. Anand R, Maheswari R, Hanefeld U (2006) Catalytic properties of the novel mesoporous aluminosilicate AlTUD-1. J Catal 242:82–91

10. Hamdy MS, Mul G, Jansen JC, Ebaid A, Shan Z, Overweg AR, Maschmeyer T (2005) Synthesis, characterization, and unique catalytic performance of the mesoporous material Fe-TUD-1 in Friedel–Crafts benzylation of benzene. Catal Today 100:255–260

11. Ramanathan A, Villalobos MCC, Kwakernaak C, Telalovic S, Hanefeld U (2008) Zr-TUD-1: a lewis acidic, three-dimensional, mesoporous, zirconium-containing catalyst. Chem Eur J 14:961–972

12. Anand R, Hamdy MS, Hanefeld U, Maschmeyer T (2004) Liquid-phase oxidation of cyclohexane over Co-TUD-1. Catal Lett 95:113–117

13. Hamdy MS, Ramanathan A, Maschmeyer T, Hanefeld U, Jansen JC (2006) Co-TUD-1: a ketone-selective catalyst for cyclohexane oxidation. Chem Eur J 12:1782–1789

14. Gorsd MN, Sathicq G, Romanelli GP, Pizzio LR, Blanco MN (2016) Tungstophosphoric acid supported on core-shell polystyrene-silica microspheres or hollow silica spheres catalyzed trisubstituted imidazole synthesis by multicomponent reaction. J Mol Catal A Chem 420:294–302

15. Heravi MM, Fard MV, Faghihi Z. (2013) Heteropoly acids-catalyzed organic reactions in water: doubly green reactions. Green Chem Lett Rev 6:282–300.

16. Misono M, Mizuno N, Katamura K, Kasai A, Konishi Y, Sakata K, Okura T, Yoneda Y (1982) Catalysis by heteropoly compounds-3. The structure and properties of 12-heteropoly acids of molybdenum and tungsten (H$_3$PMo$_{12-X}$W$_{x\ O40}$) and their salts pertinent to heterogenous catalysis. Bull Chem Soc Jpn 55:400–406

17. Shikata S, Nakata S, Okuhara T, Misono M (1997) Catalysis by heteropoly compounds. 32. Synthesis of methyltert-butyl ether catalyzed by heteropoly acids supported on silica. J Catal 166:263–271

18. Fuchs VM, Pizzio LR, Blanco MN (2008) Synthesis and characterization of aluminum or copper tungstophosphate and tungstosilicate immobilized in a polymeric blend. Eur Polym J 44:801–807

19. Gorsd MN, Pizzio LR, Blanco MN (2011) Tri-fluoromethanesulfonic acid immobilized on zirconium oxide obtained by the sol-gel method as catalyst in paraben synthesis. Appl Catal A Gen 400:91–98

20. Sosa AA, Rivera TS, Blanco MN, Pizzio LR, Romanelli GP (2013) Tungstophosphoric acid supported on zirconia: a recyclable catalyst for the green synthesis on quinoxaline derivatives under solvent-free conditions. Phosphorus Sulfur Silicon Relat Elem 188(8):10714–11079

21. Orellana MA, Osiglio L, Arnal PM, Pizzio LR (2017) Titania hollow spheres modified with tungstophosphoric acid with enhanced visible light absorption for the photodegradation of 4-chlorophenol. Photochem Photobiol Sci 16(1):46–52

22. Frenzel RA, Sathicq AG, Blanco MN, Romanelli GP, Pizzio LR (2015) Carbon-supported metal-modified lacunary tungstosilicic polyoxometallates used as catalysts in the selective oxidation of sulfides. J Mol Catal A Chem 403:27–36

23. Kapustin GI, Brueva TR, Klyachko AL, Timofeeva MN, Kulikov SM, Kozhevnikov IV (1990) A study of the acidity of heteropoly acids. Kinet Katal 3:1017–1020

24. Moffat JB, Kasztelan S (1988) The oxidation of methane on heteropolyoxometalates II. Nature and stability of the supported species. J Catal 109:206–211

25. Kasztelan S, Payen E, Moffat JB (1988) The formation of molybdosilicic acid on Mo/SiO$_2$ catalysts and its relevance to methane oxidation. J Catal 112:320–324

26. Pizzio LR, Cáceres CV, Blanco MN (1998) Acid catalysts prepared by impregnation of tungstophosphoric acid solutions on different supports. Appl Catal A Gen 167:283–294

27. Gorsd MN, Blanco MN, Pizzio LR (2016) Polystyrene/silica microspheres with core/shell structure as support of tungstophosphoric acid. Mater Chem Phys 171:281–289

28. Liu D, Quek XY, Hu S, Li L, Lim HM, Yang Y (2009) Mesostructured TUD-1 supported molybdophosphoric acid (HPMo/TUD-1) catalysts for n-heptane hydroisomerization. Catal Today 147S:51–57

29. Leofanti G, Padovan M, Tozzola G, Venturelli B (1998) Surface area and pore texture of catalysts. Catal Today 41:207

30. Brunauer S, Emmett PH, Teller E (1983) Adsorption of gases in multimolecular layers. J Chem Soc Chem 60:309–319

31. Mikhail RSh, Brunauer S, Bodor EE (1968) Investigations of a complete pore structure analysis: I. Analysis of micropores. J Colloid Interface Sci 26:45–53

32. Aquino C, Maschmeyer T (2009) A New family of mesoporous oxides—synthesis, characterisation and applications of TUD-1. In: Valentin V, Svetlana M, Michael T (eds) Ordered porous solids, recent advances and prospects, Elsevier, The Netherlands, UK, p 3–30.

33. Ranoux A, Djanashivili K, Arends IWCE, Hanefeld U (2013) B-TUD-1: a versatile mesoporous catalyst. RSC Adv 3 (44):21524–21534

34. Pizzio LR, Vázquez PG, Cáceres CV, Blanco MN (2003) Supported Keggin type heteropolycompounds for ecofriendly reactions. Appl Catal A Gen 256:125–139

35. Rocchiccioli-Deltcheff C, Thouvenot R, Franck R (1976) Spectres i.r. et Raman d'hétéropolyanions α-$XM_{12}O_{40}^{n-}$ de structure de type Keggin (X = B^{III}, Si^{IV}, Ge^{IV}, P^{V}, As^{V} et M = W^{VI} et Mo^{VI}). Spectrochim Acta A 32:587–597

36. Pizzio LR, Blanco MN (2003) Isoamyl acetate production catalyzed by $H_3PW_{12}O_{40}$ on their partially substituted Cs or K salts. Appl Catal A Gen 255:265–277

37. Chimienti ME, Pizzio LR, Cáceres CV, Blanco MN (2001) Tungstophosphoric and tungstosilicic acids on carbon as acidic catalysts. Appl Catal A Gen 208:7–19

38. Lefebvre F (1992) ^{31}P MAS-NMR study of $H_3PW_{12}O_{40}$ supported on silica: formation of $(SiOH_2^+)(H_2PW_{12}O_{40}^-)$. J Chem Soc Chem Commun 10:756–757

39. Essayem N, Tong YY, Jobic H, Vedrine JC (2000) Characterization of protonic sites in $H_3PW_{12}O_{40}$ and $Cs_{1.9}H_{1.1}PW_{12}O_{40}$: a solid-state ^{1}H, ^{2}H, ^{31}P MAS-NMR and inelastic neutron scattering study on samples prepared under standard reaction conditions. Appl Catal A Gen 194-195:109–122

40. Okuhara T, Nishimura T, Watanabe H, Na K, Misono M (1994) "Acid-base catalysis II", 4.8 novel catalysis of cesium salt of heteropoly acid and its characterization by solid-state NMR. Kodansha, Tokyo, Elsevier, Amsterdam, p 419

41. Massart R, Contant R, Fruchart J, Ciabrini J, Fournier M (1977) ^{31}P NMR studies on molybdic and tungstic heteropoly anions. Correlation between structure and chemical shift. Inorg Chem 16:2916–2921

42. Rengifo-Herrera JA, Blanco MN, Wist J, Florian P, Pizzio LR (2016) TiO_2 modified with polyoxotungstates should induce visible-light absorption and high photocatalytic activity through the formation of surface complexes. Appl Catal B Environ 189:99–109

43. Frenzel R, Morales D, Romanelli GP, Sathicq GA, Blanco MN, Pizzio LR (2016) Synthesis, characterization and catalytic evaluation of $H_3PW_{12}O_{40}$ included in acrylic acid/acrylamide polymer for the selective oxidation of sulfides. J Mol Catal A Chem 420:124–130

44. Cid R, Pecchi G (1985) Potentiometric method for determining the number and relative strength of acid sites in colored catalysts. Appl Catal 14:15–21

45. Dominguez JM, Hernandez JL, Sandoval G (2000) Surface and catalytic properties of Al_2O_3–ZrO_2 solid solutions prepared by sol–gel methods. Appl Catal A Gen 197:119–130

46. Kumar P, Pandey RK, Bodas MS, Dagade SP, Dongare MK, Ramaswamy AV (2002) Acylation of alcohols, thiols and amines with carboxylic acids catalyzed by yttria-zirconia-based Lewis acid. J Mol Catal A Chem 181:207–213

47. El-Sharkawy ESA (2006) Non aqueous titration and catalytic conversion of cyclohexanol as a test of surface acidity. Mon Chem 137:1487–1498

48. Reddy KM, Lingaiah N, Sai Prasad PS, Suryanarayana I (2006) Acidity constants of supported salts of heteropoly acids using a methodology related to the potentiometric mass titration technique. J Solut Chem 35:407–423

49. Pizzio LR, Blanco MN (2003) Isoamyl acetate production catalyzed by $H_3PW_{12}O_{40}$ on their partially substituted Cs or K salts. J Solut Chem 35:407–423